An experimental investigation on the acoustic performance of a flapping wing Micro-Air-Vehicle

Zhenbo Lu, Marco Debiasi, Quoc Viet Nguyen, Woei-Leong Chan

Temasek Laboratories, National University of Singapore, Singapore, 117411

ABSTRACT

An experimental study was conducted to assess the acoustic performance of a two-winged Flapping-Wing Micro-Air-Vehicle (FW-MAV) with various wing materials and wing structure configurations for flapping flight applications. It was concluded that highly elastic materials could significantly reduce the flapping wing noise in a wide spectrum of audible frequencies. Furthermore, a dielectric elastomer (DE) which is a lightweight and highly elastic smart material has been preliminarily investigated for its potential applications in the quiet FW-MAV under the passive control scheme.

Keywords: FW-MAV, flapping wing noise, MAV, elastic material, dielectric elastomer, passive control

1. INTRODUCTION

During the last couple of decades, there has been an increasing interest in the field of micro aerial vehicles (MAVs). The MAVs have the potential to revolutionize the sensing and information gathering capabilities in both military and civil fields. Fixed wing, rotary wing, and flapping wing [1–8] are the three main vehicle concepts. Especially FW-MAVs have very attractive characteristics for flight inside confined spaces, such as vertical take-off, slow forward flight, hovering or nearly hovering. Several research groups have been trying to develop aerial vehicles that are based on the principle of flapping flight as birds and insects. Two of the most well-known these projects are the DelFly [9-10] from TU Delft and the RoboBee [11] from Harvard University.

The aerodynamics of flapping flight are rather complex as it is highly unsteady in a low range of Reynolds number. This makes it difficult to quantify it mathematically and unlike fixed wing flight the lift cannot be straightforward calculated. In order to investigate the unsteady aerodynamic forces of flapping flight, a great deal of experimental [12-14] and numerical [15-17] studies have been conducted to understand the high-lift mechanism of the insect flight. On the contrary, the aerodynamic sound of flying insects has received less attention, although its acoustic characteristics and the associated generation mechanisms are important not only for the fundamental studies of insect physiology and evolution but also for their bio-mimetic applications.

The buzzing or bumbling sounds of bees or mosquitoes are well-known sounds generated by their flapping wings. The flapping-wing sounds are generated by flyers as a by-product of lift generation or are actively utilized for mutual communication [18-19]. The complex flow field represented by vortices such as leading edge vortex, wing tip vortex, and trailing edge vortex [20-21] which are interacting around the flapping wings generates the sound. Spatial and temporal pressure fluctuations of air are caused by this complex flow field and spreads peripherally as sound waves. It is important both biologically and technologically to clarify how these sound waves are generated and propagate. Furthermore, this can promote our understanding about the function of the motion or shape of organisms to control the sound generation which can help us to develop novel technologies to control the noise generation from bird- or insect-like FW-MAVs [22].

Due to the weight limitation of the flapping wing MAV, passive sound/noise control should be an appropriate noise control strategy for the flapping wings. In the nature, the owl has drawn a great interest for its ability to fly silently as it approaches its prey [23-24]. Researchers have observed that the owl has a special structure of combed serrations at the leading edge of its feathers that are not found from most other birds. This structure has been known to reduce noise by functioning as a vortex generator to attach the flow on the wing suction surface. A few studies investigated the effect of

leading-edge serrations on the aerodynamics of technical airfoil and found that the leading-edge serrations effectively delay the flow separation, thereby increasing the lift force and suppressing flow-induced noise [25-27]. Furthermore, it is found that bats are able to modulate the stiffness of their wing membranes for controlling their aerodynamic and acoustic performance during highly unsteady or gusty flow environments with the contraction along their wings [28-29]. Additional, the wings of some insects such as the fly and dragonfly also have hairy microstructures on their wing leading edges [30]. Therefore, it would be interesting to see if these structures on flapping wing can play a similar role in the noise reduction as the natural species.

Along this line of thinking, the objectives of the present paper are threefold: 1) Analysis on the sound/noise generation mechanism of the flapping wings; 2) Investigations on the passive/ bio-mimetic noise control strategies for suppressing flapping noise which is target to develop a quiet FW-MAV using various materials for wing fabrication, including the fabric-base wings, hyper elastic materials wings and modified geometry and configuration of wings; 3) Preliminary investigation of the bat's inspired membrane wing using dielectric elastomer film and its potential applications in the quiet flapping wing MAV under the passive control scheme.

2. FLAPPING WING MODEL AND EXPERIMENTAL CONDITIONS

2.1 Two-winged flapping-wing model

A two-winged flapping wing model was developed for the present paper base on the work done by Nguyen *et.al.* [31]. A combination of gears and conventional four-bar linkage (crank-rocker) mechanism is used in this work to create a one-degree-of-freedom flapping mechanism. The rotary motion of the motor installed into a driving gear (crank) is converted into reciprocating motion of the output link (rocker), to which the wings are attached, or flapping motion of the wings though the four-bar link.

In order to produce enough force for flight, an insect mimicking flapping-wing system should flaps at large stroke angle (at least 120 º) with wing rotation and relatively high frequency (at least 10Hz). In this flapping-wing model, the designed flapping angle of 125 º(the corresponding length of input link, coupler, and output link is 4.5 mm, 12 mm, and 5 mm, respectively), and gear ratio of 16:1 (2-stages gearbox) are chosen for fabrication of flapping-wing prototype, Fig. 1.

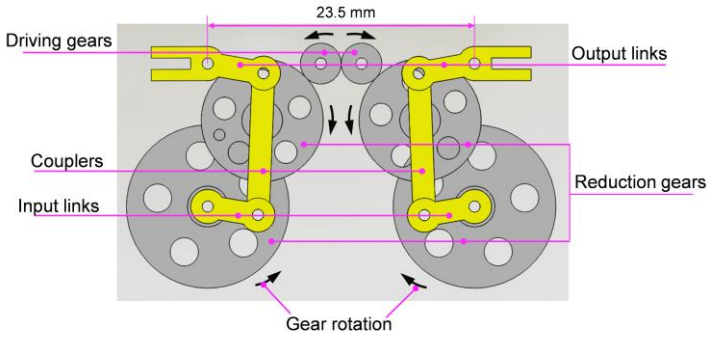

Figure 1- Flapping-wing mechanisms using 4-bar linkage (crank-rocker mechanism)

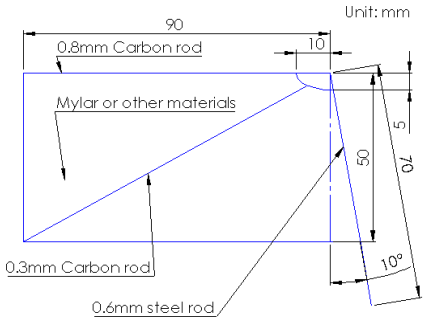

Figure 2 - The wing geometry

An AP-05 brushless motor and ESC-3 electronic speed controller (ESC) from Micronwings.com are used to drive the flapping mechanism. In this prototype, the fuselage frame is made of a carbon

tube (square section of 1.5 mm x 1.5 mm, inner hole of 1 mm, and 20 cm long). The wing span (from wing tip-to-wing tip) of the assembled model is 24cm and the weight is 11g including all electronic circuits, and 15g when installing an onboard battery.

Different types of wings were tested, Fig. 3, all of which are based on the same reference geometry shown in Fig. 2. The wing types differ in the materials used for fabricating their membranes. The properties of the different materials are summarized in Table 1 together with the denomination of the corresponding wing types. Table 1 shows that wing B made of 7 Denier Nylon non porous woven fabric has the lowest weight while wing H made of dielectric elastomer (DE) film has the largest weight. It should be noted that wing D is damaged during the measurement, thus it is not included in the present paper. Some wing types were made in more than one configuration differing from their slightly different angle of their root or by incorporating additional stiffening rods, as discussed in more detail in successive sections.

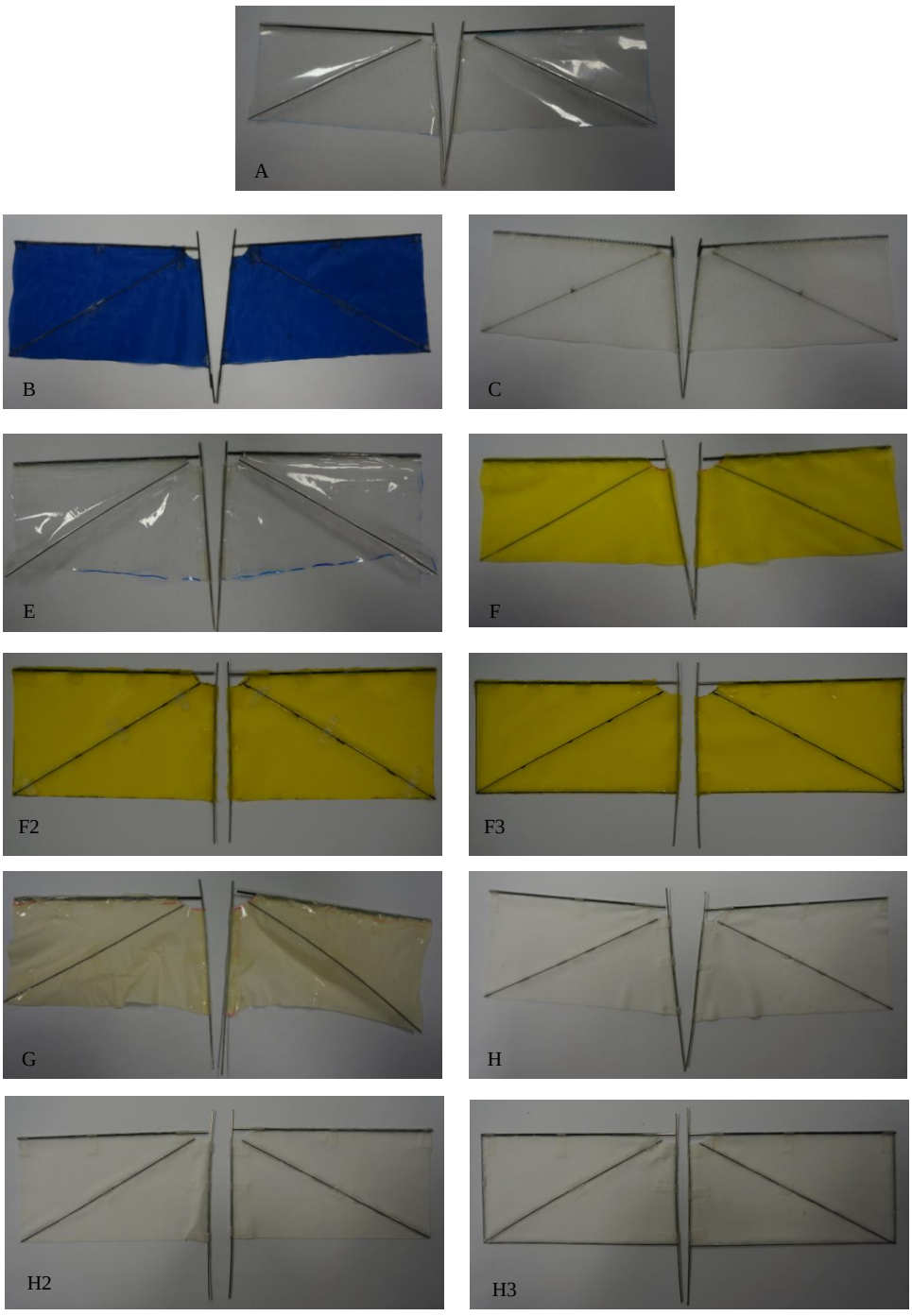

Figure 3 - Wings models A to H

Table 1- Properties of materials used the wing membrane

Type	Material	Weight*(g)	Membrane thickness (μm)
Wing A	Mylar	0.4	15
Wing B	7 Denier Nylon non-porous woven fabric	0.2	40
Wing C	porous non-woven fabric	0.6	270
Wing E	Low-density polyethylene (LDPE)	0.5	20
Wing F	Natural rubber (Oppo band)	1.1	140
Wing G	Natural rubber (Latex glove)	1.0	100
Wing H	3M VHB 4914-015 tape	1.3	150

*Inclusive the weight of the wing structure

A control box called 'pulse-width-modulation (PWM) generator and tachometer' was designed and fabricated in-house to control the brushless motor. This control box allows users to control the motor speed by turning a knob. It also determines the flapping frequency, and sends the data to a computer for display and monitoring. Furthermore, a 4.2V, 5A power supply was designed into the circuit in order to eliminate the use of one cell lithium polymer (LiPo) battery to power the electric speed controller (ESC) and motor during the experiment.

2.2 Acoustic and thrust measurement systems

Acoustic measurements were performed inside the anechoic chamber of the Temasek Laboratories at National University of Singapore (NUS). The inner dimensions of the chamber are 2350mm×2350mm×2350mm with inner walls covered by polyurethane foam acoustic wedges (Illbruck SONEXsuper) with an absorption coefficient higher than 1.0 for frequencies above 500 Hz, see Fig. 4.

The flapping wing model was installed at the center of the chamber as shown in Fig. 4. The supporting cantilever beam was firmly fixed for suppressing the influence of the vibration generated by the flapping-wing model. The front part of the flapping-wing model was hanged by a cantilever beam. With this set-up configuration, the fluid structures generated by the flapping wing can only propagate to the ground of the chamber, and therefore, it does not directly flow to the microphones. The noise was recorded by a 1/2 inch condenser microphone connected to a preamplifier and signal conditioner (Brüel & Kjær Models 4953, 2669, and NEXUS 2690-A, respectively). The microphone was rated with a response up to 15 kHz and was sampled at $f_s = 100$kHz by a fast analog-to-digital board (National Instruments PCI 6014) installed in a computer with Intel Core2 Duo 3.00GHz CPU. Each recording consisted of 10^6 samples (thus the length of the signal time trace is 10s).

The microphone was installed on a support frame that allows positioning it around the flapping-wing model, Fig. 4. In order to avoid the influences of the noise reflections from the walls, the distance between the flapping-wing model and the microphone is set to 600 mm, and the flapping wing model is hanged at 600 mm away from the floor of the anechoic chamber. A servo motor was used to rotate the frame with the microphone around the model thus allowing noise measurements along a circle whose reference angles are indicated in Fig. 11(b). Due to the symmetry of the wings and of the experimental setup, the noise from 180 º to 360 º should be the same as from 0 º to 180 º; it is only necessary to conduct measurements from 0 º to 180 º.

The signals were low-pass filtered at $f_{upper} = 0.499 f_s - 1$ (49,899Hz) by a Butterworth filter to avoid aliasing. The narrowband power spectrum of the microphone voltage was computed using a 4096-point short-time Fourier transform, which provided a spectral resolution of about 24 Hz. Using the microphone's sensitivity of 47.9 mV/Pa and accounting for the amplifier gain setting, the voltage power spectrogram was converted to the power spectrogram of p'/p_{ref}, where p' is the pressure fluctuation and $p_{ref} = 20$ μPa is the commonly used reference pressure. Converted to decibels, this becomes the spectrum of the sound pressure level $SPL(f)$, where f is the measured frequency. An A-weighting correction was applied to the SPL spectrum to account for the relative loudness perceived by the human ear. The overall sound pressure level is obtained by integrating the SPL spectrum:

$$\mathrm{OASPL} = 10log_{10}\int_0^{f_{\mathrm{upper}}} 10^{0.1SPL(f)}df \quad (1)$$

where the upper limit is the highest frequency that can be resolved, it is 15 kHz for the present case.

The average thrust of the flapping-wing model with different types of wing was measured by mounting the flapping-wing model on a 28 cm (more than 5 times higher than the wing chord) high support structure with pedestal installed on top of a AND EK-1200i balance with a range of 0g to 1200g and a resolution of 0.1g. Installing the flapping-wing model on the high structure avoided flow interactions between the flapping wings and the surfaces of the balance and of the table where it was sitting on.

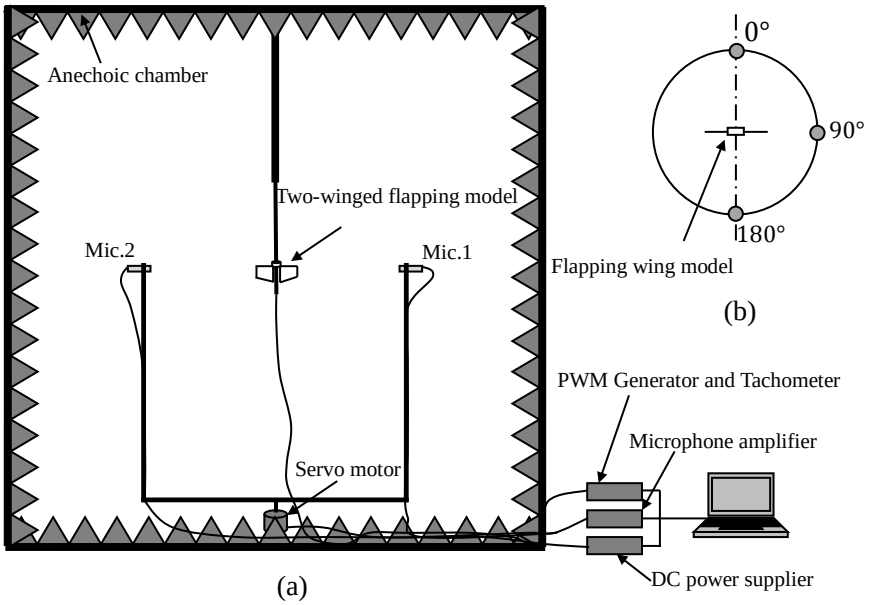

Figure 4 - The sketch of the acoustic measurement system. a) Measurement system; b) The coordination of the measurement system.

3. RESULTS AND DISCUSSIONS

The main objective of the present study is to characterize the noise generated by different wings installed on the flapping-wing model and to understand which materials and wing configurations are preferable for reducing the noise generated by the flapping-wing MAV., ideally to a level (50dBA) similar to the inside of an average house. Noise measurements were recorded at different flapping frequencies which ideally reach a maximum flapping frequency of 12 Hz; this is a typical flapping frequency of our flying flapping-wing prototypes tested in the NUS Temasek laboratories. However this flapping frequency of 12 Hz could not be reached due to the heavy weight of wings being tested. For some wings the highest flapping frequency is 10 Hz while for others are 8 Hz. Therefore, data at higher flapping frequencies up to 12 Hz was extrapolated from the measured data for each wing type. Furthermore, measurements at different angles around the flapping-wing model revealed that the peak noise propagates at an angle close to 90 °, which can be used as a reference for comparison of the acoustic characteristics since the measurements obtained at this angle are representative of the loudest, i.e., the worst case scenario, conditions.

3.1 Noise of the flapping-wing model with Mylar flapping wings

Mylar is a well-known material for flapping due its light weight and ease for wing fabrication. This material has been used to fabricate several wings for other flapping-wing prototypes developed by the NUS Temasek Laboratories as well as by other research groups around the world. Thus, we choose this material for the membrane of the reference wing (wing A) to compare with the other wings made of other materials. The Mylar membrane is flexible due to its very small thickness, but it is not highly elastic material, and thus it produces a high level noise due to wrinkling (buckling noise/popping noise) during flapping.

Figure 5a) shows the noise spectra of the flapping-wing mechanism alone (no wings) and with wing A measured at 90 ºand a flapping frequency of 8 Hz. The flapping-wing mechanism without wings is clearly quiet even if it presents three strong spectral peaks; the first peak is located at about 1100 Hz which is consistent with the frequency of 1152 Hz calculated by multiplying 9 (9 commutators inside the motor) by 128 (motor rotating speed at $8\text{Hz} \times 16$ (gear ratio)). Two high peaks appear to be its second and third harmonics. The peak at 1100 Hz is still visible with wing A. In fact its values are slightly higher, possibly indication of larger noise generated by the driving mechanisms with the load exerted by the wings. However the second and third harmonics of this peak, while still recognizable, are engulfed in the intense broadband noise produced at higher frequencies by the flapping wings.

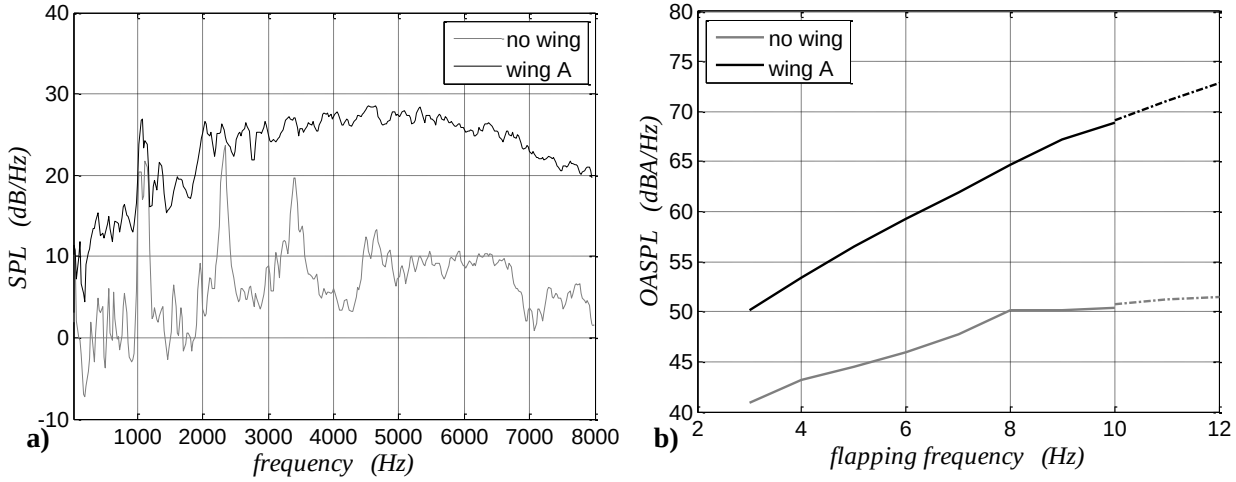

Figure 5 - Flapping-wing mechanism alone (no wing) and with type A wings: a) SPL spectra; b) OASPL values. Measurements were performed at 90 ºwith a flapping frequency of 8 Hz.

The OASPL values at 8Hz corresponding to the spectra of Fig. 5a) are 50.1dBA for the flapping-wing mechanism alone and 64.7dBA with wing A. These are visible in Fig. 5b) together with the values measured at other flapping frequencies up to 12Hz. In this figure the solid lines indicate the experimentally measured values whereas the dotted lines are the valued extrapolated for higher flapping frequencies. It is interesting to note that the noise produced by the flapping wings increases almost linearly with respect to the flapping frequency whereas that produced by the flapping-wing mechanism alone increases linearly (albeit at a lower rate) up to the flapping frequency of 8 Hz. Above this frequency the noise shows slight increase. We interpreted it as the motor and the flapping-wing mechanism approach the maximum loads they are capable to withstand above 8 Hz. Furthermore, It can be observed in the SPL spectra for flapping frequency 10Hz (figure is not shown in this paper), the increment of the noise are mainly distributing in the frequency which is ranging larger than 10000Hz. Therefore, another interpretation is that when the flapping frequency increases, the noise generated by the motor rotation also will be increased but in the higher frequency range, but the A-weighting correction curve applied in the present paper is a parabolic curve and its apex is at about 4000Hz, the increment of the noise in the higher frequency range cannot have the same weightiness as the noise in the low frequency range which lead to a lower increase rate shown in Fig. 5b). At flapping frequencies of practical interest (> 10Hz) the noise of the flapping-wing mechanism alone is marginally higher than 50dBA close to our target value for quieting a FW-MAV. On the contrary, the noise generated by wing A is about 20dBA higher than that generated by the flapping-wing mechanism alone. Thus, reducing the noise of the motor and of the flapping-wing mechanism alone is less significant than reducing the noise generated by the flapping wings which seem to be the first priority for quieting a FM-MAV. This noise reduction will be shown in the following sections which discuss the use of different materials for the fabrication of the wings as well as some structural/geometrical modifications of the wings.

3.2 Noise and thrust of the flapping-wing model with fabric-based wings

Three different types of fabric have been used for fabricating the wing membrane in an attempt to reduce the noise caused by the wrinkling of the membrane observed using Mylar. The 7 Denier Nylon is a non-porous woven fabric and it has the lowest weight of all the materials tested for the wing membrane, Table 1. The membrane of wing C is made of non-woven fabric which has porosities

passing through the material. Such passages through the fabric might allow leakage of air through the wing, thus potentially reducing its thrust performance..

The use of fabric for the fabrication of the wings' membrane is very effective for reducing the flapping-wing noise. Figure 6a) shows that using a fabric-based materials for wing membrane can reduce the flapping-wing noise of about 15dBA at flapping frequencies of practical interest. The noise produced by the FW-MAV with these fabric-based wings is about 5dBA larger than the noise measured for the flapping-wing mechanism alone. The corresponding A-weighted OASPL values per unit thrust are shown in Fig. 6b). Since the OASPL values per unit thrust are very high at low flapping frequencies, this figure presents only the values for flapping frequencies above 6 Hz, i.e., for the frequencies of practical interest. It can be observed that wing B is preferable for its lower noise signature per unit thrust than wing C in spite of its slightly worse acoustic characteristics compared to wing C. In this respect, wing C is penalized by the thrust loss caused by the air leakage through the wing membrane due to material porosities, which make its noise per unit thrust worse than even that of wing A.

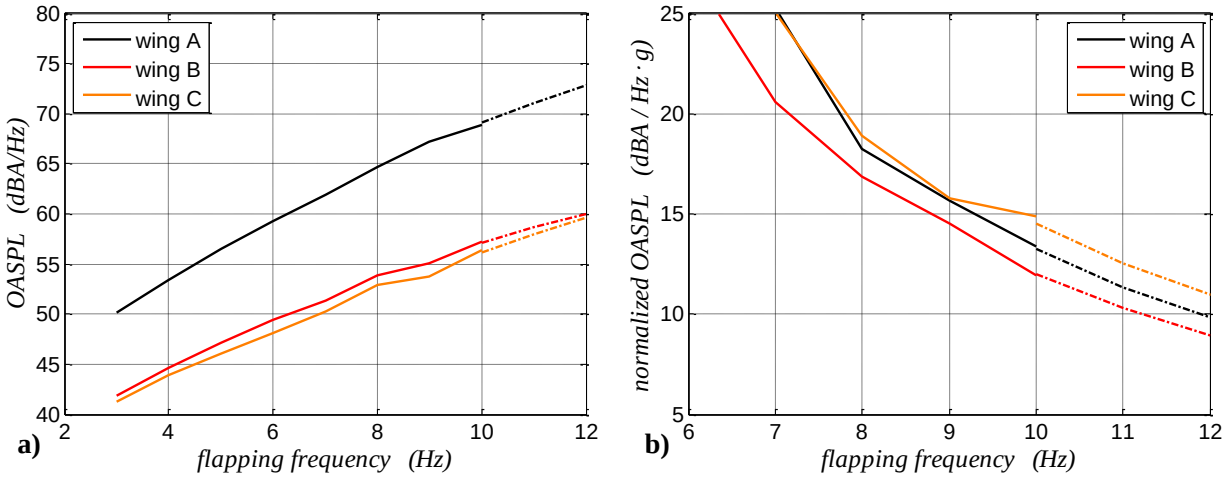

Figure 6 - Performance of wings A, B, and C: a) OASPL values; b) weighted OASPL values per unit thrust. The dashed lines are extrapolation of the data to higher flapping frequencies.

3.3 Noise and thrust of the flapping-wing model with hyper elastic materials wings

To avoid the wrinkling noise (buckling noise/popping noise) caused by the Mylar membrane of wing A during flapping, three different membranes of highly elastic materials have also been tested for fabricating the wing membrane. The membrane of wing E is made of thin and low density polyethylene (LPDE). The membranes of wing F and G are made of natural rubber which has similar characteristics to those of skin (patagium) of bats' wings and can be elastically deformed under the aerodynamic forces produced by the flapping wing. This characteristic could be exploited for tailoring or augmenting the lift characteristics of a flapping wing.

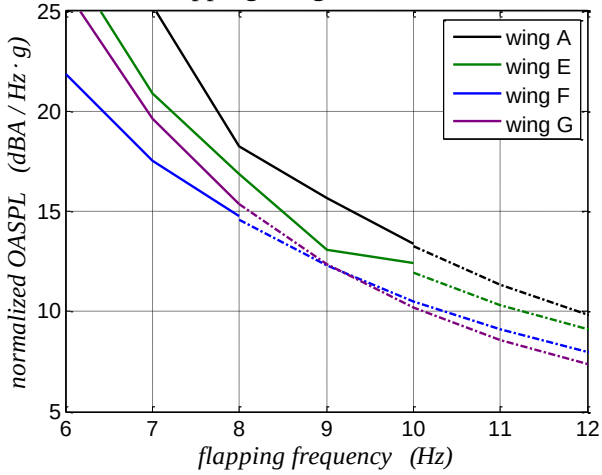

Figure 7 - OASPL values per unit thrust of wings A, E, F, and G. The dashed lines are extrapolation of the data to higher flapping frequencies.

The A-weighted OASPL values of these wings for different flapping frequencies (not shown here) indicate that wings F and G produce similar noise and have better performance than wing E. Crucially, the thrust measurements indicate that the hyper elastic-material wings produce the same or slightly higher thrust than the Mylar wing. The corresponding A-weighted OASPL values per unit thrust are shown in Fig. 7. Thanks to their higher thrust, the natural rubber wings F and G generate lower noise per unit thrust not only relative to wing A but also relative to wing B.

3.4 Noise and thrust of the flapping-wing model with wings of modified geometry and configuration

Some tests of modified wing configurations were performed for further reduction of the flapping noise. To this aim we modified the wing F with two additional configurations F2 and F3, Fig. 3. Wing F2, which does not have the 10 °degree slack angle at its root used in other wings to enable proper deformation of the wing surface, is intended to test if this simple wing configuration can produce aerodynamic force and acoustic characteristics similar to wing F. Wing F3 is inspired by the bat's membrane whose all edges reinforced with supporting ribs. We reproduced this wing by adding some flexible carbon-fibre ribs (of 0.3mm diameter) to the edges of the membrane to reduce unexpected noise generated by the inharmonious wing edge motions. The OASPL values per unit thrust are shown in Fig. 8 which indicates that original wing F already has a very low noise compared to its modified configurations: wing F2 and wing F3.

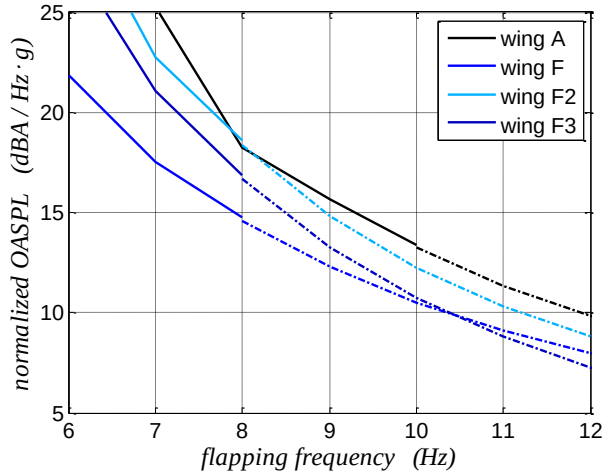

Figure 8 - A-weighted OASPL values per unit thrust of wings A, F, F2, and F3. The dashed lines are extrapolation of the data to higher flapping frequencies.

3.5 Bat's inspired membrane wing using dielectric elastomer film

The 3M VHB 4914-015 tape is one kind of dielectric elastomer (DE) film whose thickness is only 0.15mm. The acrylic form is an elastic material that feels similar to an artificial muscle or a bat's membrane wing [32-33]. Like a muscle it contracts when a voltage is applied to its surfaces, thus, its stiffness can be controlled. Therefore, it can be possible to use this material for fabricating an actively controlled membrane wing for FW-MAVs. This wing can be adjusted for obtaining high lift and low noise. Three wings H, H2, and H3 were fabricated using this material; all the three wings have same configurations as F, F2, and F3, respectively. These wings are the heaviest wings shown in Table 1. The corresponding plots of the OASPL values per unit thrust are shown in Fig. 9 indicating that the wing H has the lowest noise per unit thrust; its performance is better than that of wing A. At higher flapping frequencies it could be marginally worse than that of wings F and G shown in Fig. 7. This, coupled with the higher weight of such wings, would likely produce a noisier FW-MAV due to the larger thrust required to keep it aloft. Future experiments using the thinner and lighter 3M VHB F4960PC dielectric elastomer film may reverse this conclusion.

The wings made of dielectric elastomer film have a better acoustic performance when compared with the wings made of Mylar, up to 11.7dBA at flapping frequency 8Hz, which indicates that this novel material has great potential to be used as the wing materials of the flapping-wing model in the passive way. Furthermore, the stiffness of the pre-stretched dielectric elastomer membrane can be

adjusted by the applied voltages on its surfaces; whether the change of the stiffness of the membrane can further lead to the improvement of acoustic performance of the flapping-wing model will be studied in the future.

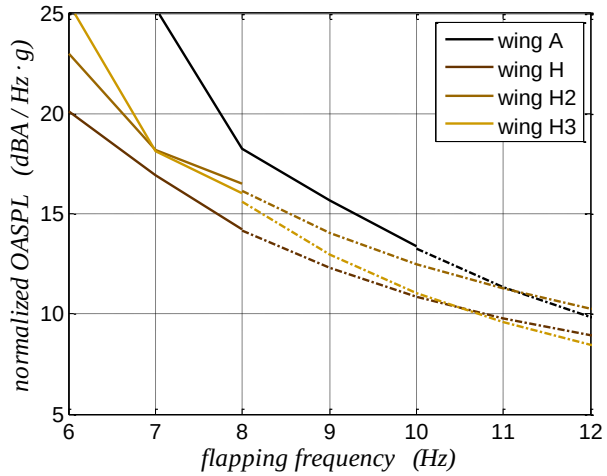

Figure 9 - A-weighted OASPL values per unit thrust of wings A, H, H2, and H3. The dashed lines are extrapolation of the data to higher flapping frequencies.

4. CONCLUSIONS

This study measured the noise characteristics of different flapping-wing configurations for MAVs with the goal of identifying guidelines for reducing their noise. Some few practical results are summarized. The best approach to reduce the noise of a FW MAV is to make it as light as possible since noise scales with the thrust required to make it fly. The use of light sheets of highly elastic materials for the fabrication of a flapping-wing membrane appears to reduce the noise produced per unit thrust of the flapping wing. All the other things being the same, higher flapping frequencies are preferable for noise reduction. This is because the thrust produced by a flapping wing increases with its flapping frequency more than the corresponding noise. Based on the limited tests conducted it is not possible to draw a conclusion on the benefits of geometrical modifications of a flapping wing for noise reduction. Effective geometrical and structural modification may be possible if these will be based on a clear understanding of the physics of their noise production.

Dielectric elastomer (DE) films for the fabrication of a wing membrane appear to be a very attractive as these materials would allow tailoring the mechanical properties of the membrane. However, such materials per se do not seem to produce quieter flapping wings than the elastic materials. Additional experiments with thinner DE films are required to further assess this point.

REFERENCES

1. W. Shyy, Y.Lian, J. Tang, D. Viieru and H. Liu, “Aerodynamics of low Reynolds number flyers,” NewYork, Cambridge University Press, 2008.
2. W. Shyy, M. Berg and D. Ljungqvist, “Flapping and flexible wings for biological and micro air vehicles,” Prog. Aerosp. Sci, 1999, 35(5), pp. 455–505.
3. T. J. Muller, Fixed and flapping wing aerodynamics for micro air vehicle applications. AIAA Prog Astronaut Aeronaut, 2001, 195.
4. W. Shyy, P. Ifju,D. Viieru, “Membrane wing-based micro air vehicles,” Appl. Mech. Rev, 2005, Vol. 58, pp. 283–301.
5. D. J. Pines, F. Bohorquez, “Challenges facing future micro-air-vehicle development,” J. Aircraft, 2006, Vol. 43(2), pp. 290–305.
6. M. Platzer, K. Jones, J. Young and J. Lai, “Flapping wing aerodynamics:progress and challenges,” AIAA J, 2008, Vol. 46(9), pp.2136–2149.
7. Y. Lian, W. Shyy, D. Viieru, B. Zhang, “Membrane wing aerodynamics for micro air vehicles,” Prog. Aerosp. Sci, 2003, Vol. 39(6-7), pp. 425–465.

8. B. K. Stanford, P. Ifju, R. Albertani, W. Shyy, “Fixed membrane wings for micro air vehicles: experimental characterization, numerical modelling and tailoring,” Prog. Aerosp. Sci, 2008, Vol. 44(4), pp. 258–294.
9. Samir Saberi, “From Insectothopter to Dely,” TU Delta, 2008.
10. de Croon, G.C.H.E., de Clerq, K.M.E., Ruijsink, R., Remes, B., and deWagter, C., “Design, aerodynamics, and vision-based control of the DelFly,” The International Journal on Micro Air Vehicles, Volume 1, Number 2, pp. 71- 97, 2009.
11. B. Finio, B. Eum, C. Oland, and R.J. Wood, “Asymmetric apping for a robotic y using a hybrid power-control actuator,” IEEE/RSJ IROS, St. Louis, MO, Oct., 2009.
12. C. P. Ellington, C. van den Berg, A. P. Willmott, and A. L. R. Thomas, “Leading-edge vortices in insect flight,” Nature (London) 384, 626–630, 1996.
13. J. M. Birch and M. H. Dickinson, “Spanwise flow and the attachment of the leading-edge vortex on insect wings,” Nature (London) 412, 729–733, 2001.
14. M. H. Dickinson, F. O. Lehmann, and S. P. Sane, “Wing rotation and the aerodynamic basis of insect flight,” Science 284, 1954–1961, 1999.
15. Z. J. Wang, “Two dimensional mechanism for insect hovering,” Phys. Rev. Lett. 85, 2216–2219, 2000.
16. M. Sun and J. Tang, “Unsteady aerodynamic force generation by a model fruit fly wing in flapping motion,” J. Exp. Biol. 205, 55–70, 2002.
17. M. Sun and J. Tang, “Lift and power requirements of hovering flight in drosophila,” J. Exp. Biol. 205, 2413–2427, 2002.
18. S. Drosopoulos and M. F. Claridge (ed), “Insect sound and communication, Physiology, Behavior, Ecology, and Evolution, CRC press, Taylor and Francis Group, Florida, USA, 2006.
19. J. Sueur, E. J. Tuck and D. Robert, “Sound radiation around a flying fly”, J. Acoust. Soc. Am., Vol. 118(1), 2005, pp. 530-538.
20. C. Van den Berg and C. P. Ellington, “The vortex wake of ‘hovering’ model hawkmoth,” Phil. Trans. R. Soc. Lond., B352, 1997, pp. 317-328.
21. S. P. Sane, “The aerodynamics of insect flight,” J. Exp. Biol. Vol. 206, 2003, pp. 4191-4208.
22. T. J. Mueller, “Fixed and flapping wing aerodynamics for micro air vehicle applications,” Progress in Astronautics and Aeronautics, Vol. 195, 2001.
23. R. R. Graham, “The silent flight of owls,” J. R. Aeronaut. Soc. 286, 837 (1934).
24. G. M. Lilley, “A study of the silent flight of the owl,” AIAA Paper No. 98-2340, 1998.
25. A. S. Hersh, P. T. Soderman, and R. E. Hayden, “Investigation of acoustic effects of leading-edge serrations on airfoils,”J. Aircraft 11, 197 (1974).
26. R. E. A. Arndt and R. T. Nagel, “Effect of leading-edge serrations on noise reduction from a model rotor,” AIAA Paper, No. 72-655, 1972.
27. S. Ito, “Aerodynamic influence of leading-edge serrations on an airfoil in a low Reynolds number – A study of an owl wing with leading edge serrations,” J. Biomech. Sci. Eng. 4, 117 (2009).
28. Swartz, S. M., Groves, M. S., Kim, H. D., and Walsh, W. R., “Mechanical properties of bat wing membrane skin,” Journal of Zoology, Vol. 239, 1996, pp. 357–378.
29. Swartz, S. M., Bishop, K. L., and Ismael-Aguirre, M. F., “Dynamic complexity of wing form in bats: implications for flight performance,” Functional and evolutionary ecology of bats, edited by Z. Akbar, G. McCracken, and T. H. Kunz, Oxford University Press, xford, U. K., 2005, pp. 110–130
30. B. G. Newman, S. B. Savage, and D. Schouella, “Model tests on a wing section of an Aeschna dragonfly,” in Scale Effects in Animal Locomotion, edited by T. J. Pedley (Academic, London, 1977), pp. 445–477.
31. Quoc Viet Nguyen, Chan Woei Leong, and Marco Debiasi, “Design, Fabrication, and Performance Test of a Hovering-Based Flapping-Wing Micro Air Vehicle Capable of Sustained and Controlled Flight,” 2014 International Micro Air Vehicle Conference and Competition (IMAV 2014), August 12-15, 2014 Delft, The Netherlands.
32. Pelrine, R., R., K., Pei, Q., and Joseph, J., “High-Speed Electrically Actuated Elastomers with Strain Greater Than 100%,” Science, Vol. 287, No. 5454, 2000, pp. 836–839.
33. O’Halloran, A., O’Malley, F., and McHugh, P., “A review on dielectric elastomer actuators, technology, applications, and challenges,” Journal of Applied Physics, Vol. 104, No. 071101, 2008.